



Electrochemical influence of Aminobenzene on the pitting corrosion behaviour of Type 304 stainless steel in dilute sulphuric acid

R.T. Loto^{1,2,*} and I. Akinwumi³

¹Department of Mechanical Engineering, Covenant University, Ota, Ogun State, Nigeria

²Department of Chemical, Metallurgical & Materials Engineering, Tshwane University of Technology, Pretoria, South Africa

³Department of Civil Engineering, Covenant University, Ota, Ogun State, Nigeria;

Received 23 June 2014, Revised 5 July 2014, Accepted 6 July 2014

*Corresponding Author. E-mail: tolu.loto@gmail.com ; Tel: (+2348084283392)

Abstract

The electrochemical influence of aminobenzene (AMB) concentrations on the pitting corrosion resistance of austenitic stainless steel type 304 in 3M sulphuric solutions with 3.5% sodium chloride addition was evaluated through potentiodynamic polarization technique. The pitting potential, passivation potential, passivation range, nucleation resistance and passivation capacity were analyzed with respect to specific aminobenzene concentrations. Under impressed potential difference the stainless steels in acid solution acquired a passive state, with breakdown at the transpassive region (pitting potential), however this was greatly increased to higher values with aminobenzene addition causing significant increase in the passivation range and potentials greatly higher than the value that necessitates pitting in the acid media due to enhanced corrosion resistance of the stainless steel through formation of protective film of aminobenzene molecules. The results obtained establish the dynamic relationship and interaction between the aminobenzene concentration and electrochemical parameters in the corrosion behavior of the stainless steel at ambient temperature of 25 °C.

Keywords: corrosion, organic compound, electrochemical technique, nucleation

1. Introduction

Stainless steel passivation is due to the adsorption of oxygen on the steel surface as a result of bond formation between its uncoupled d electrons and oxygen atoms [1, 2]. This hinders the electrochemical kinetics responsible for corrosion. However adsorption of electronegative ions responsible for corrosion coupled with simultaneous displacement of oxygen atoms results in insidious corruptions such as pitting. Pitting corrosion initiation and propagation is subject to factors responsible for any electrochemical reaction such as charge-transfer mechanisms, ohmic effects and mass transport phenomena [3, 4]. The importance of environmental and material factors relevant to the pitting process, such as electrochemical potential, alloy composition, electrolyte concentration and temperature can be understood by their role on pit growth stability. Influence of the passive film characteristics and the mechanism of the initiation of pitting or breakdown of the otherwise protective passive film are highly important in the study of pitting corrosion. Pitting corrosion is a complex but important problem at the root of many corrosion failures. It has been studied in detail for many years yet the crucial phenomena remains unclear [5 - 12]. This investigation aims to evaluate the electrochemical influence of aminobenzene (AMB) on the pitting corrosion inhibition of austenitic stainless steel in high molar sulphuric acid contaminated with sodium chloride.

2. Experimental Methods

2.1 Material

Commercially available Type 304 austenitic stainless steel was used for all experiments of average nominal composition; 18.11%Cr, 8.32%Ni and 68.32%Fe. The material is cylindrical with a diameter of 18mm.

2.2 Inhibitor

Aminobenzene (AMB) a brownish, translucent liquid obtained from SMM instruments, South Africa is the inhibitor used. The structural formula of AMB is shown in fig. 1. The molecular formula is $C_6H_5NH_2$ while the molar mass is 93.13 gmol^{-1} .

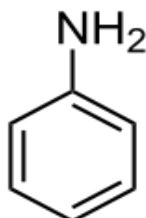


Figure 1: Chemical structure of Aminobenzene (AMB)

AMB was prepared in concentrations of 1.25%, 2.5%, 3.75%, 5%, 6.25% and 7.5% per 200 ml of the acid media.

2.3 Test Media

3M sulphuric acid with 3.5% recrystallized sodium chloride of analar grade were used as the corrosion test media.

2.4 Preparation of Test Specimens

The cylindrical stainless steel (18mm dia.) was mechanically cut into a number of test specimens of dimensions in length ranging from 17.8mm and 18.8mm coupons. The two surface ends of each of the specimen were ground with Silicon carbide abrasive papers of 80, 120, 220, 800 and 1000 grits. They were then polished with $6\mu\text{m}$ to $1\mu\text{m}$ diamond paste, washed with distilled water, rinsed with acetone, dried and stored in a desiccator for linear polarization test.

2.5 Linear Polarization Resistance

Linear polarization measurements were carried out using, a cylindrical coupon embedded in resin plastic mounts with exposed surface of 254 mm^2 . The electrode was polished with different grades of silicon carbide paper, polished to $6\mu\text{m}$, rinsed by distilled water and dried with acetone. The studies were performed at ambient temperature with Autolab PGSTAT 30 ECO CHIMIE potentiostat and electrode cell containing 200 ml of electrolyte, with and without inhibitor. A graphite rod was used as the auxiliary electrode and silver chloride electrode (SCE) was used as the reference electrode. The steady state open circuit potential (OCP) was noted. The potentiodynamic studies were then made from -1.5V versus OCP to $+1.5 \text{ mV}$ versus OCP at a scan rate of 0.00166V/s and the corrosion currents were registered. The corrosion current density (j_{cr}) and corrosion potential (E_{cr}) were determined from the Tafel plots of potential versus log I . The corrosion rate (R), the degree of surface coverage (θ) and the percentage inhibition efficiency ($\%IE$) were calculated as follows

$$R = \frac{0.00327 \times I_{cr} \times E_q}{D} \quad (1)$$

Where I_{cr} is the current density in $\mu\text{A/cm}^2$, D is the density in g/cm^3 ; E_q is the specimen equivalent weight in grams. The percentage inhibition efficiency ($\%IE$) was calculated from corrosion rate values using the equation.

$$\%IE = 1 - \left[\frac{R_2}{R_1} \right] \times 100 \quad (2)$$

where R_1 and R_2 are the corrosion rates in absence and presence of inhibitors, respectively.

3. Results and discussion

3.1 Introduction

Figure 2 is a representative diagram of the variation of potential E with log current density for austenitic stainless steel in the dilute sulphuric acid/chloride media.

- AB represents cathodic reaction.
- BG is the represents anodic dissolution reaction. The metal is not passivated at the corrosion potential (E_{cr} , B).
- AC and DC are Tafel straight lines
- At potentials more positive than B, corrosion rate increases, and reaches a maximum at the passivation potential, G, which is often given the symbol, E_{pp} .
- The transition from active dissolution occurs in the region G to J. A protective film begins to form and causes a sudden drop in corrosion current density.
- From J to P, the passive zone, the current density is maintained steadily, until point P
- At P (pitting potential E_{pit}), breakdown of the protective film begins. It is here that the likelihood of pitting is greatest, and consequently specimen failure.
- E_{pit} often called the critical pitting or breakdown potential is a useful parameter in assessing pitting properties of materials. It should be noted that it is not an absolute parameter, and varies according to both metallurgical and electrochemical conditions.
- At potentials more positive than P, the current density begins to rise as more and more pits propagate [13].

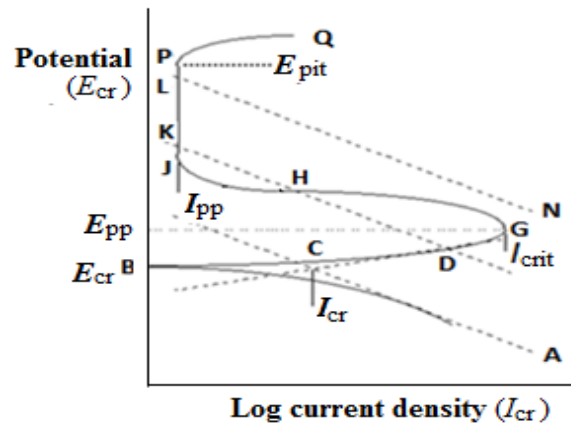


Figure 2: Representative diagram of the variation of potential E with log current density

3.2 Specimen Analysis (Sample A – G)

Observation of Table 1 shows the near linear relationship between AMB concentrations and corrosion rates due to decreased electrolytic action caused by the activity of AMB inhibiting cations. This reduces the anodic dissolution and hydrogen evolution reactions. In localized corrosion, the rate of anodic reaction usually varies with position along the corroding surface owing to variations in potential, alloy composition and solution concentration within pitted regions. Sample A showed the highest corrosion rate while sample G showed the lowest due to the electrochemical action of AMB compound at maximum concentration, thus the higher the concentration of AMB, the lower corrosion rate. The polarization resistance of the samples varied considerably with decrease in corrosion current density accompanied by alternating values of cathodic and anodic Tafel constants indicating differential redox reactions with respective to AMB concentration. This observation is responsible for passivation of the stainless steel at region (J-P) (fig. 2), due to the protective film offered by the AMB compound. The corrosion rate shows a specimen whose resistance to corrosion in the acid media is enhanced by the inhibiting effect of AMB.

The corrosion rate for sample A is due to applied potential without AMB addition. The chloride and sulphate anions in solution migrate to the metal/oxide interface and form a metal chloride phase complex that cracks the overlying oxide as a result of its larger specific volume. This provides a ready source of anions to initiate and stabilize pit growth from the onset. The combined chloride and sulphate ions in sample A, solution undoubtedly caused more deleterious degradation on the stainless steel compared to other samples, the

consequence of which was that of severe active corrosion reactions of anodic dissolution of the control sample. In the presence of the reacting species, (Cl^- and SO_4^{2-}), the ability of the stainless steel to repair its protective film was drastically reduced and the protection was lost. The relative concentration of metal cations within the pit solution increases with increase in chloride/sulphate concentration which results in increase in the dissolution rate of the steel. At region P-Q ~ (fig. 2) the anions significantly aggravates the conditions for formation and growth of the pits, beginning at specific areas (regions of film breakage or weakness due to the presence of impurities and inclusion). Galvanic coupling is established between these discontinuous zones, which form small anodes. Through an autocatalytic process the gradually formed pits becomes continuously loaded with positive metal ions because of anodic dissociation. The Cl^- ions concentrates in the pits for charge neutrality and encourage the reaction of positive metal ions with water to form a hydroxide corrosion product and H^+ ions which combine to release hydrogen gas. At this region the passive film is electrochemically unstable, undergoing potential-dependent transpassive dissolution. Progression from the passive state to pitting phase can also be explained on the basis of competitive adsorption interaction between the corrosive anions and the elemental atoms responsible for passivity whereby corrosive anions migrate to the metal/liquid interface resulting from an impressed current sequentially reaching the critical potential (E_{pit}), i.e. the pitting potential which corresponds to the Cl^- concentration necessary to displace adsorbed oxygen species and facilitate the oxidation of iron atoms. The more noble the E_{pit} obtained at a fixed potential, the less susceptible the material to the initiation of localized corrosion [13]. The E_{pit} for austenitic stainless steel occurs at the point when the anodic current increases sharply. The presence of adsorbed Cl^- increases the potential difference across the passive film thereby enhancing the rate of Fe^{2+} diffusion from the metal/film interface to film/solution interface. Studies of the structure of the passive film on stainless steels have shown that the properties of steels are due to the selective dissolution of chromium metal and accumulation of Chromium (III) oxide (Cr_2O_3) on the passive film [14].

Table 1: Data obtained from polarization resistance measurements for austenitic stainless steel in 3M H_2SO_4 in presence of AMB compound

Sample	Inhibitor Concentration (%)	b_a (V/dec)	b_c (V/dec)	E_{cr} (V)	j_{cr} (A/cm ²)	i_{cr} (A)	Corrosion Rate (mm/year)	R_p (Ω)	Inhibition Efficiency (%)
A	0	0.980	0.740	-0.322	7.74E-02	1.97E-01	7.95	1.615	0
B	1.25	0.115	0.133	0.328	2.08E-03	5.28E-03	2.13	1.258	73.18
C	2.5	0.127	0.080	-0.328	1.04E-03	2.64E-03	1.07	1.673	86.54
D	3.75	0.024	0.057	-0.326	9.89E-05	2.52E-04	1.02	2.418	87.22
E	5	0.730	0.094	-0.410	1.09E-03	2.77E-03	1.12	1.075	85.91
F	6.25	0.460	0.034	0.329	1.06E-04	2.71E-04	1.09	2.486	86.25
G	7.5	0.049	0.048	0.325	1.08E-04	2.74E-04	1.11	3.573	86.10

The polarization curve in fig.2 shows a spontaneously passive material, meaning that the protective passive film is present on the metal surface at different passivation potentials (E_{pp} , region G). During upward scanning, breakdown occurs, and a stable pit starts growing at the E_{pit} which proceeds in the transpassive region of the polarization curve, here the current increases sharply from the passive current level. The understanding of the passive film as being self activating, instead of a rigged structure, is critical to the indepth knowledge of the mechanisms of passive film breakdown and pit initiation. This can be assessed under three mechanisms such as passive film penetration, film breaking and adsorption mechanism. The penetration mechanism involves the diffusion chlorides and sulphates from the electrolyte through the passive layer to the oxide/metal interface under the influence of the high electrical field strength of most passivating films.

The film-breaking mechanism starts with cracks in the passive layer under induced corrosion activity, exposing small areas of bare metal surface to the electrolyte and the related very intense metal dissolution that leads to the formation of pits. The adsorption mechanism refers to agitated electrochemical diffusion of metallic cations from the passive film to the electrolyte due to the reactivity of corrosive ions and chromium depletion causing the collapse of the passive film. It's possible that nucleation event develops into the second phase of pit formation, i.e. the metastable pit growth (region J-P). This phase ceases if the pit repassivates. Inhomogeneities

on the surface of the alloy are initiation sites for pit formation. In certain cases, metastable pitting develops and the process moves almost immediately to the stage of stable pit growth i.e. pit propagation. During the pit propagation stage, active dissolution of the metal matrix takes place continuously in the pit.

The necessary condition for an active pit is the presence of an aggressive environment inside the pit. Under this condition, the pit remains active, behaving as a small anode, while the surrounding surface acts as a large cathode. The rapid production of metal ions within the pit induces the diffusion and migration of anions such as Cl⁻ chiefly responsible for breakdown of the passive film. Breakdown of the passive film can be seen partially dependent of the circumstances associated with pitting corrosion. At a particular potential the passive film perforates due to anion adsorption. The steel sample is said to be in a transpassive condition at which dissolution initiates and gradually progress as shown in fig. 3. Once a pit nucleates, metal dissolution self-propagates causing the film to lose its capacity to repassivates as observed in the transpassive region of the polarization curves. Once a pit is formed, corrosion products are formed and accumulate within the pit, and they destroy passivity wherever contact is made with the alloy surface resulting in a rapid increase in the number of active pitting sites. That corrosion product has a high ionic conductivity, resulting in a higher corrosion rate in the pits in contrast to the remaining areas that are passive. The Cl⁻ ions can diffuses through the passive film defects and flaws with the assistance of high electric field across the passive film to reach the base metal surface and accelerate the local anodic dissolution.

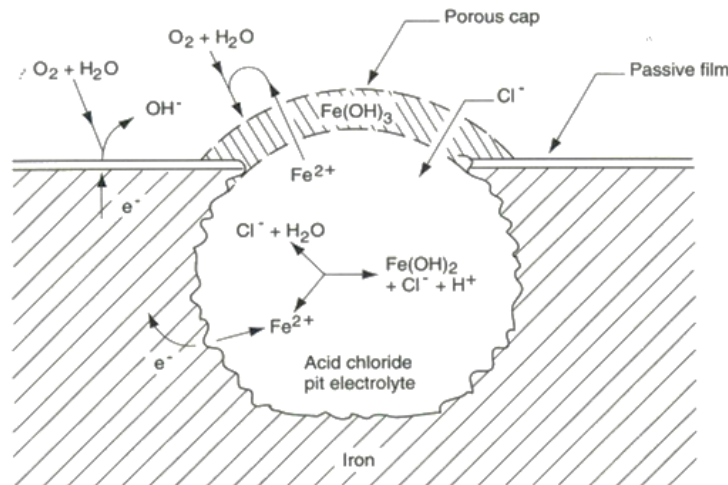


Figure 3: Schematic of processes occurring in an actively growing pit

3.3 Influence of AMB Compound on the pitting corrosion of austenitic stainless steel.

The potentiostatic values for the pitting corrosion of austenitic stainless steel in 3M H₂SO₄ at specific concentrations of AMB compound is shown in Table 2. The pitting potential value (E_{pit}) increased with increasing AMB concentration from sample A to D due to the action of AMB molecules and amine functional groups (NH³⁺). At sample E there was a substantial decrease in the pitting potential till sample G, despite the increase in inhibition efficiency and a progressive decrease in corrosion rate, AMB was unable to sustain its pitting resistance ability probably due to lateral repulsion between the inhibitor molecules which allows for partial diffusion of chlorides and sulphates, due to slight weakening of its protective film. The pitting potential values are further upset by the passivation potential, i.e. the potential at which the steel passivates after subduing metastable pitting. This value shows the ability of the steel to quickly passivate forming the protective film. The passivation potential values in Table 2 shows a steel specimen where AMB delays the onset of passivation progressively with increase in AMB concentration i.e. its delays the formation of the passivating film necessary for the increased pitting corrosion resistance of the steel. The passivation range and nucleation capacity of the specimen shows declining values after sample D, which shows that AMB at high concentrations thins out the passivating film of the steel specimen, but results of passivation capacity (passivation potential with respect to E_{cr} values) shows a material with a strong tendency to passivate after 5% AMB.

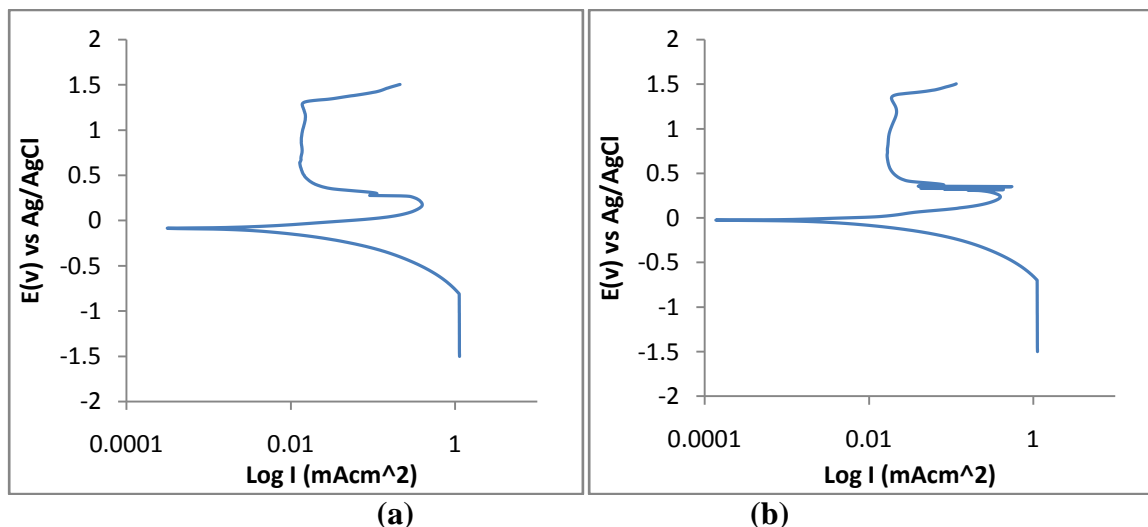
Table 2: Potentiostatic values of ASS in 3M H₂SO₄ solution/AMB

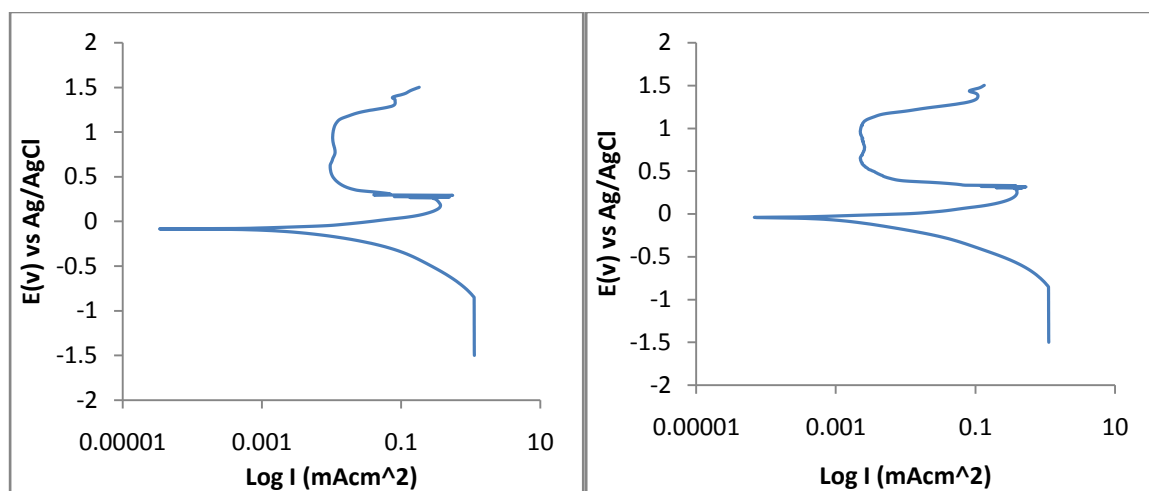
Sample	Inhibitor Concentration (C)	Pitting Potential (v)	passivation Potential (v)	Passivation Range (v)	Nucleation Resistance (v)	passivation Capacity (v)
A	0	1.210	0.384	0.826	1.532	0.706
B	0.000268	1.239	0.331	0.908	1.567	0.659
C	0.000537	1.274	0.366	0.908	1.602	0.694
D	0.000805	1.317	0.399	0.918	1.643	0.725
E	0.001074	1.171	0.448	0.723	1.581	0.858
F	0.001342	1.166	0.502	0.664	0.837	0.173
G	0.001611	1.151	0.668	0.483	0.826	0.343

Pitting occurred at a higher potential due to the reduced influence of chloride and sulphate ions by AMB adsorption onto the metal oxide. At E_{pit} , the initiation of pitting could be ascribed to competitive adsorption between SO_4^{2-}/Cl^- ions due to breakage or chemical modification of the protective film at high potentials. The SO_4^{2-}/Cl^- ions displace the adsorbed AMB cations at some locations, thus penetrating it under high electric field across the film and accelerate localized anodic dissolution. Increase in AMB concentration shifts the value of E_{pit} to more positive potentials commensurate with an increase in the alloy resistance to corrosion. The passivation capacity values proves the alloy to be highly resistant and durable to pitting corrosion in the presence of AMB as increase in AMB results in significant decrease in passivation capacity values after sample E, thus the enhanced alloy passivity, due to film formation by chemisorption with the inhibitor molecules heights.

3.4 Nucleation Resistance, Passivation Capacity, Passivation Range and Passivation Potential

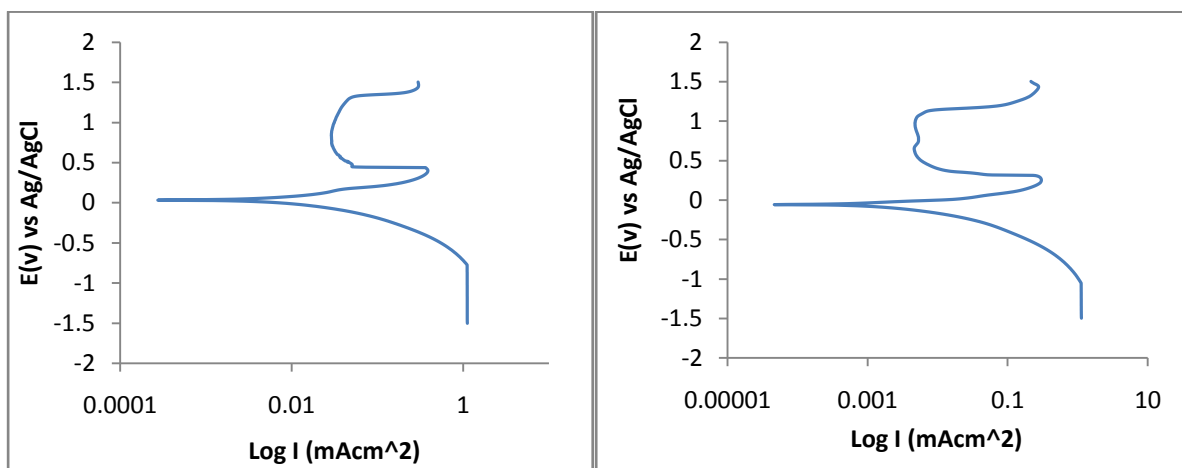
The corrosion within the pits is anodic surrounded by a large cathode area. The anodic process is sustained autocatalytically due to the high concentration of metal and corrosive anions in addition to high concentrations of hydrogen ions due to hydrolysis. Passive metals are susceptible to localized attack by pitting when polarized above a certain potential in the electrolytic solution. The anions destroy the passive layer by preferential adsorption. These ions are attracted to the metal, and compete with oxygen and any other passivating agent, for adsorption on the metal surface. The process results in substitution of adsorbed oxygen. Due to high reactivity between the metal/chloride interactions the metal rapidly deteriorates first at specific areas of defects before propagating to the entire surface. The result is pitting, often observed when passive metals corrode. Delayed pit formation is partly due to competitive adsorption. AMB cations also tend to adsorb on the alloy surface slightly displacing the corrosive anions at low concentration. This causes positive E_{cr} displacement.





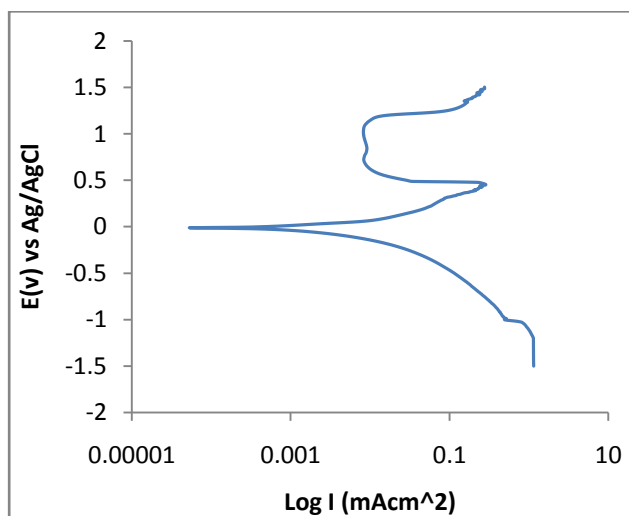
(c)

(d)



(e)

(f)



(g)

Figure 4(a-g): Polarization Curve of austenitic stainless steel (0% - 75% AMB) in 3M H₂SO₄

The pit nucleation resistance NR ($E_{\text{pit}} - E_{\text{cr}}$), passivation range ($E_{\text{pit}} - E_{\text{pp}}$) and passivation capacity PC ($E_{\text{pp}} - E_{\text{cr}}$) can be considered to be a measure of the susceptibility of alloys to pitting corrosion [15, 16]. Alloys exhibiting higher values of nucleation resistance and lower values of passivation capacity are more resistant to pitting corrosion. Nucleation occurrence is because of the creation and evolution of metastable pits. These pits form and develop for short period before passivation, at potentials well beneath the pitting potential and during the induction time before the onset of stable pitting at potentials above the pitting potential. Nucleation symbolizes the breakdown and passivation of the passive film and occurs extremely rapidly. Current increase depicts the initiation and progression of pits while the instantaneous decrease represents passivation and pit termination. Specific accumulation of chloride and sulphate complexes results in the formation of meta-soluble precipitate on the metal surface. This hampers the stability of the passive film at lower to higher potentials. The sequential hysteresis in current value depicts the sequential breakage and formation of occlusions during metastability which increases the porosity of the covering. The difference between NR and CR for the polarization curves shows the passivation range (Table 2) (fig. 2, region B-J). There is a sharp reduction in the passivation rate in the acid solutions due to the inability of the stainless steel to sustain its passive state, thus failure occurs at lower potentials. The presence of a high concentration of adsorbed chloride ions at these sites will of course prevent further growth of the passive film and result in the establishment of active pits.

3.5 Scanning Electron Microscopy Analysis

The micrograph (fig. 5a) shows topography with perforations and micropits under high magnification consisting of sulphur and chloride residues. These anions are responsible for the formation of pits leading to pitting corrosion. The sulphate and chloride ions cause the release and ionic diffusion of iron cations beyond the metal solution interface into the acid solution. This results in the accelerated deterioration and corrosion of the stainless steel alloy, eventually causing alloy dissolution and pit growth. The topography in (fig. 5b) is the product of accumulation of AMB molecules due to their deposition on the steel surface. This is due to the adsorption of the molecules of AMB, resulting from electrostatic attraction with the surface of the steel. The corrosive species are displaced from the steel surface through competitive adsorption and simultaneously prevented from reaching the surface due to the protective barrier formed.

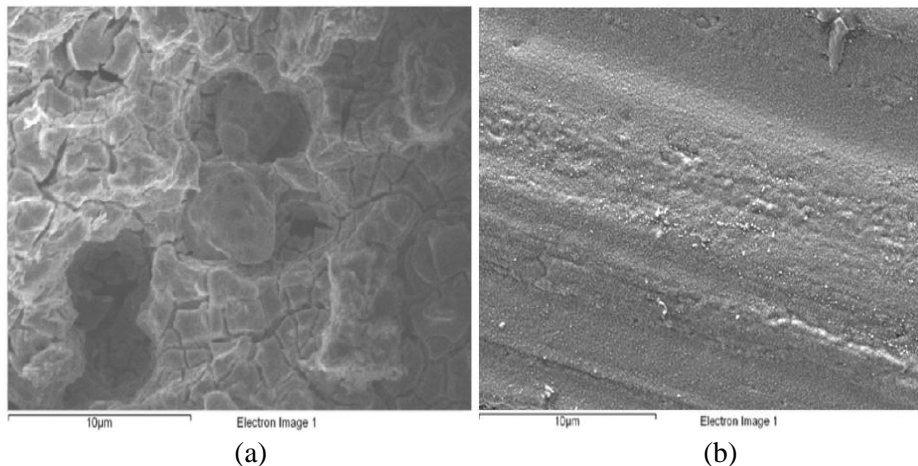


Figure 5: SEM micrographs of: a) Austenitic stainless steel in 3M H₂SO₄, b) Austenitic stainless steel in 3M H₂SO₄ with AMB.

3.6 Passivity Studies

The passive film formed on the stainless steels is composed of chemical combination of iron and chromium oxides in addition to hydroxides and oxyhydroxides. At the onset of passivation there is a chemical reaction between metal cations and water to form hydrated species resulting in the formation of the oxide film by de-protonation of the hydroxyl ion [17]. Under anodic polarization the stainless steel samples acquired a passive state, with breakdown at the transpassive potential (fig.2 and fig. 4). The plots in fig. 4 demonstrate similar anodic

behaviour of the steels within the passive range, regardless of the absence and presence of chloride and sulphate ions. This fact may be attributed to the similarity of the passive films. The variation in parameters characterizing anodic passivity (the passivation current density and the passivation potential) and the widths of the passive region is due to the action of chloride and sulphate ions as its concentration increases. The presence of chloride ions in the sulphuric acid solution causes a sharp current increase at potentials significantly lower than those of transpassivity. The current increase causes breakdown and perforation of the passive film which reduces the passive potential range.

Pitting corrosion is induced by the attack of the anions diffused into the passive film through electrochemical migration under the electrostatic influence [18]. The electrolytic transport of the anions through the film is due to the selective nature of the layer on the passive film in the solution. The anions accumulate in the region leading to the formation of pits [19]. During pit initiation, the passive film is bombarded and attacked by the chloride and sulphate ions causing breakdown mostly at specific sites e.g. non-metallic solutions, impurities etc. This results in hysteresis in current density due to anion adsorption. Under this circumstance the electrostatic intensity at the boundary layer reaches a critical value corresponding to the pitting potential. In the acid solutions with AMB addition there is competition for adsorption between the anions and AMB cations, the passivation effect of AMB at low concentration is small but as the concentration increases there is a resultant effect whereby the steel is effectively protected from anion attack through film formation by AMB cations which reduces the concentration of iron cations in the acid solutions. This process aids the chromium aggregates at the metal/oxide interface thereby reinforcing the passivation characteristics of the metal specimen slowing down or virtually stopping the metal dissolution process.

3.7 Influence of Oxygen

Pit nucleates on ferrous alloys in the absence of oxygen. Oxygen depletion prevents the production of hydroxyl ions [20-22]. This electrochemical mechanism causes the accumulation of ionized metal atoms on the surface creating strong electrostatic affinity from the chloride anions resulting in the accelerated metal dissolution within the pit [23]. Stainless steels are unable to repassivate in the absence of oxygen in addition to reciprocal alterations which depletes the protective film. Naturally oxygen reacts with metal cations from the anodic dissolution process to form protective oxides on the metal interface. This reduces anodic oxidation responsible for corrosion. Lack of oxygen supply causes the propagation and progression of pits. Under induced corrosion, the impressed current evokes the diffusion of chloride species to the pit interior, destroying the passive film in the process, thereby accelerating the mechanism of corrosion reaction.

Conclusion

The electrochemical influence of aminobenzene on the pitting corrosion resistance of austenitic stainless steel was investigated in dilute sulphuric acid contaminated with sodium chloride salts. Comparison of polarization curves and tables from the electrochemical tests with differential AMB concentrations in sulphuric acid solution shows the compound significantly increase the potential necessary for pit initiation, thus enhancing the steels resistance to pitting corrosion as a result of the inhibitory effect of AMB which displaces the anions of chlorides and sulphates through competitive adsorption, forming a compact impenetrable protective film on the steel surface. Results and observation show an increase in the passive regions in the sulphuric acid/sodium chloride media with AMB concentration compared to the control acid solution as the rate of repassivation occurs faster than the reaction mechanisms requires for pit formation and propagation.

Acknowledgement-The authors acknowledge the Department of Chemical, Metallurgical and Materials Engineering, Faculty of Engineering and the Built Environment, Tshwane University of Technology, Pretoria, South Africa for the provision of research facilities for this work.

References

1. Uhlig H. H. *J. Elect. Soc.* 5(100) (1953) 216
2. Stern S. *J. of Elect. Soc.* 11(105) (1958) 638
3. Fregonese M., Idrissi H., Mazille H., Renaud L., Cetre Y. *Corros. Sci.* 4(43) (2001) 627.

4. Prošek T., Novák P. *Mats and Corr.* 12(54) (2003) 933.
5. Gouda V.K., AbdElMeguid E.A. *12th International Corrosion Congress*, Texas, USA, (1994)
6. Wang J.H., Su C.C., Szklarska-Smialowska Z. *Corrosion*, 44(1988)732
7. AbdElMeguid E.A., Gouda V.K., Mahmoud N.A. *Materials Transactions, JIM.*, 35(1994)703
8. Gouda V.K., Hashem A. *International Conference on Advances in Corrosion and Protection.* (1992).
9. AbdElMeguid E. A., Mahmoud N. A., Gouda V. K. *British Corrosion J.*, 32(1997) 68
10. AbdElMeguid E.A. *Corrosion.* 53(1997)623
11. AbdElMeguid E. *J.Mats.Sci.* 33(1998) 3465
12. Ashour E.A., AbdElMeguid E.A., Ateya B.G. *Corrosion.* 53(1997)612
13. Loto. R. T. *J. Mater. Environ. Sci.* 4 (4) (2013) 448
14. Olsson C.O.A., Landolt D. *Electrochimica Acta*, 48 (2003)1093
15. Ajit, K.M., Balasubramaniam, R. *Mats Chem. & Phys* 103(2-3)(2007) 385
16. Lihua, Z., Wei, Z., Yiming, J., Bo, G., Daoming, S., Jin, L. *Electrochimica Acta*, 54 (23) (2009) 5387
17. Olefjord I., Brox B. *in proceedings of the 5th international symposium on passivity of metals and semiconductors.* Société de Chimie Physique. Elsevier science publishers. Amsterdam, 561(1983)
18. Mohammed A. A., Nader El Bagoury, Adel A. O, Adel S. M. *Int. J. Electrochem. Sci.*, 7(2012) 2643
19. Frankel G. S., Sridha N. *Mater. Today.* 11 (2008) 38-44
20. Aballe A., Bethencourt M., Botana F.J., Cano M.J., Marcos. *Corros. Sci.*, 2001, 43(2001)1657
21. Smailowska Z. S. *Corros. Sci.*, 41(1999)1743
22. Barbucci A., Bruzzone G. *Intermetallics*, 8 (2000) 305.
23. Pietro P. M. *Fatigue and Corrosion in Metals*, Springer Science & Business Media, (2012) 660

(2015); <http://www.jmaterenvironsci.com>